

Evolution of active galactic nuclei broad-line region clouds: low- and high-ionization lines

D.R. Gonçalves^{1,2}, A.C.S. Friaça² and V. Jatenco-Pereira²

¹ Instituto de Astrofísica de Canarias, C. Via Láctea s/n, E-38200 La Laguna - Tenerife, Spain

² Instituto Astronômico e Geofísico - USP, Av. Miguel Stefano 4200, 04301-904 São Paulo - SP, Brazil

denise@ll.iac.es, amancio@iagusp.usp.br, jatenco@iagusp.usp.br

ABSTRACT

The formation of quasar broad-line region (BLR) clouds via thermal instability in the presence of Alfvén heating has been discussed by Gonçalves et al. (1993a, 1996). In particular, these studies showed the relevance of Alfvén heating in establishing the stability of BLR clouds in the intercloud medium. The present paper shows the results of time-dependent calculations (we use a time-dependent hydrodynamic code) following the evolution of BLR clouds, since their formation from the 10⁷ K intercloud medium. We also calculate the UV and optical line emission associated with the clouds in order to compare with observations. Our results are compared with those of UV and optical monitoring of well-studied AGN, which suggest that the BLR is most probably composed of at least two different regions, each one giving rise to a kind of line variability, since low- and high-ionization lines present different patterns of variability. We discuss the alternative scenario in which lines of different ionization could be formed at the same place but heated/excited by distinct mechanisms, considering as a non-radiative mechanism the Alfvén heating.

Key words: Quasars: BLR – Hydrodynamics – Plasma: Alfvén heating – Emission-line variability

1 INTRODUCTION

The study of the broad-line regions (BLR) of active galactic nuclei (AGN) is crucial in understanding the central engine of these objects. In addition, as the BLR reprocesses energy emitted by the continuum source at ionizing ultraviolet energies that cannot be observed directly, the monitoring of emission lines provides unique pieces of information on the central continuum source. Photoionization by continuum radiation from the central source is almost certainly the most important heating/ionizing mechanism in BLRs. One should note that non-thermal processes, for instance incoherent synchrotron radiation, were earlier invoked to explain AGN spectra (for instance, Rees 1984, 1987; Contini & Viegas-Aldrovandi 1990). In any case, the pure photoionization model has a number of inconsistencies — the ‘energy budget problem’, the ‘line ratio problem’ and the ‘line variation problem’ (Dumont, Collin-Souffrin & Nazarova 1998). In fact, Dumont et al. (1998) speculate on the need and nature of a non-radiative heating source of energy — dissipation of sound or Alfvén waves, weak shocks, magnetic dissipation, etc., as a possibility to partially solve these problems. The non-radiative process discussed here is the interaction between Alfvén waves, which results in a dissipation process heating the gas. The present study aims at evaluating

the effects of Alvenic heating (AH) as non-radiative heating, in addition to pure photoionization, on the broad-line spectrum.

We studied two damping mechanisms for Alfvén waves: the nonlinear and turbulent. These damping mechanisms have been investigated before, showing the relevance of Alfvén waves and their dissipation processes in all the following astrophysical objects. Late-type and proto stars (Jatenco-Pereira & Opher 1989a, b; Vasconcelos, Jatenco-Pereira & Opher 2000); solar wind (Jatenco-Pereira & Opher 1989c; Jatenco-Pereira, Opher & Yamamoto 1994); galactic and extragalactic jets (Opher & Pereira 1986; Gonçalves, Jatenco-Pereira & Opher 1993b); early-type stars (dos Santos, Jatenco-Pereira & Opher 1993; Gonçalves, Jatenco-Pereira & Opher 1998); broad line regions of quasars (Gonçalves, Jatenco-Pereira & Opher 1993a, 1996); and finally, optical filaments in cooling flows (Friaça et al. 1997).

The scenario for BLRs considered in this article is the two-phase BLR, in which the optical–UV lines are emitted by clouds embedded in a hot, external, intercloud medium (Krolik, McKee & Tarter 1981). However, thermal pressure alone is not enough to confine BLR clouds if the external medium is heated only by Compton scattering (Mathews & Ferland 1987; Mathews & Doane 1990). Mathews & Doane (1990) take into consideration various physical

processes in the heating–cooling the BLR, including: i) recombination heating and cooling; ii) radiative losses in the range between 10^4 K to 3×10^7 K due to the electron excitation of resonance transitions in the commonest metal ions; iii) thermal Bremsstrahlung; and iv) Compton heating–cooling. They conclude that thermal instability cannot form the quasar line-emitting clouds for the observed pressure $P \sim 10^{-2}$ dyne cm $^{-2}$. On the other hand, magnetic fields and intense radiation may provide an important contribution to the formation and confinement of the clouds (Rees 1987; Gonçalves et al. 1993a, 1996). The additional heat source considered here, AH, together with more conventional ones (see Mathews & Ferland 1987; Krolik 1988; Mathews & Doane 1990), maintain the broad-line emitting clouds and the intercloud medium in pressure equilibrium (Gonçalves et al. 1993a, 1996), as required in the two-phase BLR model (see Netzer 1990). Within the framework of our model, the correlation between continuum and line emission of the BLR is also affected by AH as an additional heating/excitation source of the BLR, acting together with photoionization by the central source.

The present study extends the stationary equilibrium calculations of Gonçalves et al. (1993a, 1996, hereafter Papers I and II, respectively), in which it was found that AH could establish a stable two-phase medium in BLRs, by performing time-dependent calculations for the evolution of line-emitting clouds from their formation from a 10^7 K intercloud gas to $\sim 10^4$ K clouds. We compare the results of our models with observational data coming from optical and UV AGN monitoring campaigns.

Section 2 reviews the knowledge of magnetic fields in BLRs and the AH mechanisms. The time-dependent models for BLR clouds are discussed in Section 3. Model results and their comparison with the observations of AGN UV and optical lines are given in Section 4. An overall discussion as well our main conclusions are stated in Section 5.

2 ALFVÉN HEATING IN THE BLR INTERCLOUD MEDIUM

The classical observational signature of magnetic fields in AGN is the radio emission resulting from synchrotron radiation of relativistic electrons spiralling in a magnetic field. Rees (1987), considering the magnetic confinement of BLR clouds, has estimated a magnetic field strength of ~ 1 G, in the inner parsec of AGN (this value refers to the hot intercloud gas). Since magnetic field are present in BLRs, we also expect the existence of Alfvén waves. On disturbing a uniform magnetic field, the magnetic tension makes a wave propagate along the field lines with the Alfvén speed, v_A (for a review see Priest 1994). The perturbations of the magnetic fields could originate in the central region of the AGN, which is highly perturbed as we infer from the fast continuum variability. Therefore, two conditions that are fulfilled by the central region of AGN make them favourable sites for the generation of Alfvén waves: they contain magnetic fields and are highly perturbed.

The diagnosis of the basic physical parameters of BLRs is not simple because electron densities are high enough for almost all forbidden lines to be collisionally suppressed. However, the temperature is estimated via similarity with

other ionized gases, with temperatures of about 10^4 K. The characteristic broad-line widths are ~ 5000 km s $^{-1}$, but the above temperature implies a line-of-sight velocity dispersion of ~ 10 km s $^{-1}$! Therefore, line widths do not reflect thermal motions only, but are also due to bulk motions of individual broad-line emitting clouds. These clouds are ‘usually assumed, without justification, to have no turbulent velocity’ (cf. Baldwin 1997). On the other hand, the clouds could not be highly turbulent since in this case the effects on the line asymmetries would be enormous. The blue and red asymmetries of the broad lines are usually explained by infall or outflow, but we are still far from a complete explanation of these features (see Espy 1997 for a brief review of velocity diagnostics in BLRs). Therefore, the line widths reveal the existence of bulk motions and, possibly, of turbulence in the BLR, thus fulfilling the conditions for the BLR to produce Alfvén waves.

Once we admit the existence of Alfvén waves in the AGN BLRs, the Alfvén waves are subject to several damping processes. In this work we consider the nonlinear and the turbulent damping processes. Assuming spherical geometry for the clouds, we present below the dependence of the Alfvén wave heating rate on density and temperature (see Papers I and II for a detailed discussion).

High amplitude waves cause nonlinear mode couplings and, in this process, the resulting modes are rapidly damped. In general, the waves that result from the damping processes are sound waves; thus, the nonlinear Alvenic energy is converted into thermal energy. An Alfvén wave is likely to dissipate because of its nonlinear interaction with either a non-uniform ambient field or another Alfvén wave (Wentzel 1974). The nonlinear interaction of magnetohydrodynamic waves has been treated in detail by Kaburaki & Uchida (1971), Chin & Wentzel (1972) and Uchida & Kaburaki (1974). In regions of strong ($v_A > c_s$) magnetic field, one Alfvén wave can decay into another Alfvén wave and a sound wave travelling in the opposite direction. The resulting Alfvén wave has a frequency smaller than the original one and it can, in turn, decay into another lower-frequency Alfvén wave plus an acoustic wave. The cascade continues until all the Alvenic energy has been converted to acoustic waves that dissipate rapidly. Considering this mechanism, in our models, the onset of AH occurs for $\beta = (B^2/8\pi)/n k_B T > \beta_{\text{on}} > 1$, where β_{on} is the initial value of β when AH becomes important ($\beta > 1$ corresponds to $v_A/c_s > \sqrt{6/5}$ for an ideal $\gamma = 5/3$ gas, where c_s is the sound speed). Note that our definition of β corresponds, in a plane parallel geometry, to $\beta = p_B/p_{\text{gas}}$, whereas in plasma physics, $\beta_{\text{pl}} = p_{\text{gas}}/p_B$ denotes the ‘ β parameter’ of the plasma. The present convention for β has been widely used in cooling flow studies (e.g. David & Bregman 1989), and has been employed by Friaça et al. (1997) in the study of the effects of AH in optical filaments in cooling flows.

According to Lagage & Cesarsky (1983), the nonlinear damping rate is

$$\Gamma_{\text{nl}} = \frac{1}{4} \sqrt{\frac{\pi}{2}} \xi \bar{\omega} \left(\frac{c_s}{v_A} \right) \frac{\rho \langle \delta v^2 \rangle}{B^2/8\pi}, \quad (1)$$

where $\xi = 5 - 10$, $\bar{\omega}$ is the characteristic Alfvén frequency and $\rho \langle \delta v^2 \rangle / (B^2/8\pi)$ the ratio of the energy density of Alfvén waves to that of the magnetic field. In laboratory plasmas, the cut-off frequency of Alfvén waves is often comparable to

the ion-cyclotron frequency, $\omega_{ci} = eB/m_ic$, so we can write $\bar{\omega}$ as a fraction F of ω_{ci} , i.e., $\bar{\omega} = F\omega_{ci}$. In addition, there are experimental grounds to set $F \approx 0.1$ or smaller (Burke, Maggs & Morales 1998).

In terms of AH, e.g. H_{nl} (erg cm⁻³ s⁻¹), we have: $H_{nl} = (\Phi_w \Gamma_{nl})/v_A$, where Φ_w is the wave flux, Γ_{nl} is given by (1), and v_A is $B/\sqrt{4\pi\rho}$. As the perturbation collapses, the component of the magnetic field perpendicular to the direction of compression is amplified. For spherical geometry $B \propto A^{-1} \propto \rho^{2/3}$, where A is the cross-sectional area perpendicular to the magnetic field. As a consequence, $v_A \propto \rho^{1/6}$. Let the dependence of Φ_w on ρ be given by $\Phi_w \propto A^{-1} \propto \rho^{2/3}$. Taking $\Phi_w = \rho\langle\delta v^2\rangle v_A$, we have $\rho\langle\delta v^2\rangle \propto \rho^{1/2}$. Since $c_s \propto T^{1/2}$, for \bar{w} independent of the density, we obtain:

$$H_{nl} \propto \rho^{-1/2} T^{1/2}. \quad (2)$$

In addition, the nonlinear interaction between outward and inward propagating waves results in an energy cascading process (Tu, Pu & Wei 1984). Following Hollweg (1986, 1987), the volumetric heating rate associated with the cascade process (e.g. associated with turbulent damping of Alfvén waves) can be written as

$$H_{tu} = \rho\langle\delta v^2\rangle^{3/2} / L_{corr}, \quad (3)$$

where L_{corr} is a measure of the transverse correlation length of the magnetic field. Again, for spherical geometry, $\langle\delta v^2\rangle \propto \rho^{1/2-1} \propto \rho^{-1/2}$, and adopting $L_{corr} \propto B^{-1/2} \propto \rho^{-1/3}$, we obtain:

$$H_{tu} \propto \rho^{7/12}. \quad (4)$$

We would like to call the reader's attention to the fact that Paper II has a misprint in equations (4) and (6), more specifically, in the dependence of Φ_w on the density (in the calculations the correct expression was used). Equations (2) and (4) now exhibit the right dependence of Φ_w on the density. As a matter of fact, these heuristically derived density dependencies were included in Paper II, since we have discussed not only AH density dependency due to nonlinear, resonance surface and turbulent Alfvénic dampings, but also a range of other density dependencies for "like-Alfvénic heatings" (see Fig. 9 of Paper II). In the other two papers discussing AH in other environments than those of BLRs, the correct expressions for H_{nl} and H_{tu} are found (Friaça et al. 1997; Gonçalves, Jatenco-Pereira & Opher 1998).

3 TIME-DEPENDENT COOLING CONDENSATIONS

We have investigated the evolution of quasar BLR clouds from their formation out of the hot phase of the BLR and calculated their ultraviolet and optical signatures within the scenario outlined in Section 2. The evolution of the cooling clouds is obtained by solving the hydrodynamic equations for mass, momentum and energy conservation (see Friaça 1986, 1993):

$$\frac{\partial \rho}{\partial t} + \frac{1}{r^2} \frac{\partial}{\partial r} (r^2 \rho u) = 0 \quad (5)$$

$$\frac{\partial u}{\partial t} + u \frac{\partial u}{\partial r} = -\frac{1}{\rho} \frac{\partial p_t}{\partial r} - \frac{GM(r)}{r^2} \quad (6)$$

$$\begin{aligned} \frac{\partial U}{\partial t} + u \frac{\partial U}{\partial r} &= \frac{p_t}{\rho^2} \left(\frac{\partial \rho}{\partial t} + u \frac{\partial \rho}{\partial r} \right) - \Lambda \rho + \frac{H(\rho, T)}{\rho} \\ &+ \frac{1}{\rho r^2} \frac{\partial}{\partial r} \left(\kappa r^2 \frac{\partial T}{\partial r} \right) \end{aligned} \quad (7)$$

where u , ρ , p_t , U , T and κ are the gas velocity, density, total pressure, the specific internal energy, temperature, and the thermal conductivity coefficient. The equation of state,

$$U = \frac{3}{2} \frac{k_B T}{\mu m_H} + \frac{u_B}{\rho} \quad (8)$$

relates U to T and $u_B = B^2/8\pi$, the internal magnetic energy density (k_B is the Boltzmann's constant, m_H is the hydrogen atomic mass and $\mu = 0.62$ is the mean molecular weight of a fully ionized gas with solar abundances).

The total pressure, p_t , is the sum of the thermal and magnetic pressures, $p_t = p + p_B$. The constraints on the magnetic pressure come from considerations on the β -parameter, assuming that the magnetic pressure of the unperturbed medium would not exceed its thermal pressure, in accordance with Mathews & Doane (1990). We assume frozen-in fields tangled on scales less than that of the perturbation, so that, for spherical collapse, $B \propto \rho^{2/3}$ ($p_B \propto \rho^{4/3}$). In this case the magnetic field can be considered as effectively isotropic and we treat the isotropic tangled magnetic field as a $\gamma = 4/3$ gas, and so $p_B = u_B/3 = B^2/24\pi$.

The self-gravity of the condensations is taken into account through $M(r)$, the mass distribution of the gas. Note, however, that the self-gravity is much less important than the tidal force due to the BH, as one can see from the comparison between the surface gravity of the perturbation (of mass $M = 4\pi\rho_m R^3$ and radius $R = L/2$ for the values of ρ_m and L defined in the next section)

$$g_{suf} = GM/R^2 = 8.4 \times 10^{-8} \text{ cm s}^{-1}$$

and the tidal acceleration due to a central supermassive black hole of mass $M_{BH} = 10^8 M_\odot$ at a distance $r = 30$ light-days of the perturbation:

$$g_{tid} = GM_{BH}R/r^3 = 0.71 \text{ cm s}^{-1}.$$

In the energy equation, the heating term $H(\rho, T)$ follows either equation (2) or equation (4) and it is turned off in the case of no heating. In the adopted definition of the cooling function $\Lambda(T)$, $\Lambda(T)\rho^2$, is the cooling rate per unit volume. Since there is no ionization equilibrium for temperatures lower than 10^6 K, the ionization state of the gas at $T < 10^6$ K is obtained by solving the time-dependent ionization equations for all ionic species of H, He, C, N, O, Ne, Mg, Si, S, Ar and Fe. The radiative cooling function was obtained via the collisional ionization code MEKA (Mewe, Gronenschild & van der Oord 1985). The coefficients of collisional ionization, recombination and charge exchange of the ionization equations is also from MEKA. The adopted abundances are cosmic abundances usually assumed in AGN models (Netzer 1990). If solar abundances are used, they are taken from Grevesse & Anders (1989).

The last term of eq. 7 accounts for the thermal conductivity. We take the thermal conductivity coefficient, κ , as a fraction, η , of the Spitzer (1956) value $\kappa_S = 4.87 \times 10^{-7}$ erg cm⁻¹ K⁻¹, with $\eta = 10^{-4}$. The thermal conductivity should be inhibited, otherwise it would prevent the

development of the thermal instability. The thermal conductivity would erase any steep temperature gradient arising in the medium, thus heating the cooler gas of BLRs to the higher temperatures of the surrounding hot gas. Therefore, the presence of colder clouds embedded in a hot gas requires some reduction of the thermal conduction. A similar inhibition of thermal conduction seems to be needed also in cooling flows in clusters of galaxies: the classic (Spitzer) thermal conductivity would drive a heat flow towards the cooling flow, and, as a consequence, there should be no cooling flow! The magnetic fields could be at the origin of the inhibition of thermal conductivity. In the presence of magnetic fields, the heat conduction is suppressed in the direction perpendicular to the magnetic field, taking place substantially only along magnetic field lines. If the magnetic field is very tangled, the heat conduction can be reduced by a large factor. Other processes of inhibition of thermal conductivity besides magnetic field entanglement are possible. For instance, in cooling flows in galactic clusters, electromagnetic instabilities driven by temperature gradients (or electric currents in other situations) can also cause this inhibition, even for non-tangled field lines (Pistinner, Levinson & Eichler 1996).

The spherically symmetric hydrodynamical equations are solved using a finite-difference, implicit code based on Cloutman (1980). The code is run in the Lagrangian mode and the grid points are initially spaced logarithmically, with a grid of 100 cells. The artificial viscosity for the treatment of the shocks follows the formulation of Tsharnutter & Winkler (1979) based on the Navier-Stokes equation. In contrast with the von Neumann-Richtmyer artificial viscosity (Richtmyer & Morton 1967), this form of artificial viscosity vanishes for homologous contraction. Thermal conduction is included by operator-splitting using a Crank-Nicholson scheme. The outer boundary conditions on pressure and density are derived by including an outer fictitious cell, the density and pressure in which are obtained from extrapolation of power laws over the radius fitted to the outermost real cells.

The initial density perturbations are characterized by an amplitude, A , and a length scale, L , following

$$\delta\rho = \frac{A \sin(x)}{x} ; \quad x = \frac{2\pi r}{L} . \quad (9)$$

We have also assumed that the perturbations are isobaric and nonlinear ($A=1$), avoiding the uncertainties concerning the linear development of thermally unstable modes in the presence of a gravitational field (David, Bregman & Seab 1988). The unperturbed hot-phase intercloud medium is characterized by a total hydrogen density $n_m = 5 \times 10^6 \text{ cm}^{-3}$ and a temperature $T_m = 10^7 \text{ K}$, appropriate for the inner regions of an AGN, $\sim 10^{18} \text{ cm}$ from the central source, where lies the BLR. If the gas cools isobarically, when it reaches $T = 10^4 \text{ K}$, the resulting central electronic density would be $6 \times 10^9 \text{ cm}^{-3}$, consistent with the absence of forbidden line emission in AGN BLRs. We fixed $\beta_0 = B^2/(8\pi n k_B T_m) = 0.03$ in accordance with Mathews & Doane (1990) who pointed out that this quantity should be between 0.003 and 0.03, in a similar calculation with no Alfvénic heating. The length scale of the perturbation was fixed at $5 \times 10^{16} \text{ cm}$. The corresponding column density is $N_H = 3.2 \times 10^{23} \text{ cm}^{-2}$.

Here we investigate several representative models with magnetic fields, one with no AH and the others with AH

due to two damping mechanisms (nonlinear and turbulent) and at different efficiencies (see Table 1). Model I allows for the presence of a magnetic field only through a magnetic pressure term in the equation of motion. In models II and III, the energy equation includes AH as an additional heating term. We considered nonlinear and turbulent Alfvén wave heating, from the above equations (eqs. (2) and (4)), and these heating terms have the forms

$$H_{\text{nl}} = \zeta H_0 (n/n_0)^{-1/2} (T/T_0)^{1/2} , \quad (10)$$

for nonlinear heating, and

$$H_{\text{tu}} = \zeta H_0 (n/n_0)^{7/12} , \quad (11)$$

for turbulent heating, where ζ is the efficiency of Alfvén heating. The choice of the normalization is the following: 1) $T_0 = 10^5 \text{ K}$ (the temperature at which optical emission begins to be important); 2) $n_0 = 13.59 \times (5 \times 10^6) \text{ cm}^{-3}$, where 13.59 would be the compression factor from the unperturbed $n_m = 5 \times 10^6 \text{ cm}^{-3}$ and $T_m = 10^7 \text{ K}$ initial state to $T = T_0$, under isobaric conditions for a plane parallel geometry; and 3) $H_0 = (3/2) n_0 k_B T / t_{\text{col}} \text{ erg cm}^{-3} \text{ s}^{-1}$, where t_{col} is the collapse time (defined below) for the cloud with no Alfvénic heating.

4 MODELLING RESULTS AND DATA COMPARISON

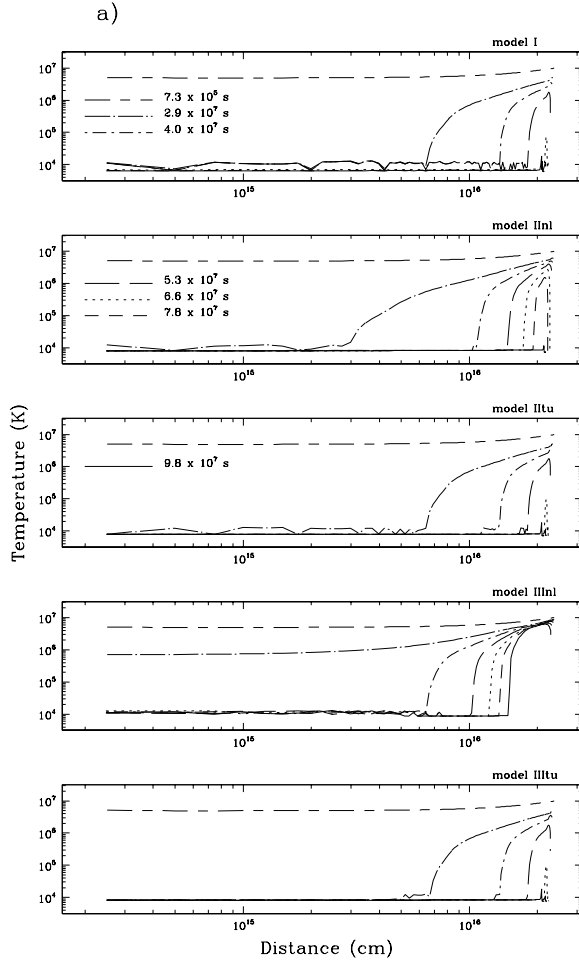
We investigate models with magnetic field and AH (excepted model I in which there is no AH) using H_{nl} and H_{tu} with the efficiency of the conversion of Alfvén wave energy in Alfvénic heating, ζ , equivalent to 10% and 30%. In model I the magnetic effect is considered only as magnetic pressure in the equation of motion. All the other models contain AH as an additional heating term in the energy equation. The characteristics of our models are summarized in Table 1: model identification (column 1); the Alfvénic heating considered in each model (column 2); the efficiency ζ of the AH (column 3); and the total collapse time $t_{\text{t,col}}$, i.e. the time since the beginning of the calculations until the time when the innermost cell reaches $8 \times 10^3 \text{ K}$ (column 4).

First of all, note that AH can maintain stable equilibrium between the optical line-emitting cloud and the inter-cloud medium. In fact, Friaça et al. (1997), studying the Alfvén heating/excitation of the optical filaments in cooling flows, have found that one of their models (with nonlinear heating and $\zeta = 100\%$) reached thermal stability, showing that AH can suppress strong growth of thermal instabilities in cooling flows. This suggests that AH could induce a stable two-phase equilibrium in other astrophysical environments, such as the BLRs of AGN, which were investigated with simple time-independent calculations in Papers I and II. Therefore, we take the initial conditions of our simulations from Paper II. As we see from Table 1, an increase in the AH efficiency from 10% to 30%, leads to longer total collapse times: from 10.10 to $10.60 \times 10^7 \text{ s}$ for the models with H_{nl} and from 9.89 to $9.93 \times 10^7 \text{ s}$ for those with H_{tu} . The same trend of collapse time with ζ was found by Friaça et al. (1997), thus confirming that AH inhibits development of thermal instabilities.

Figure 1 -3 show the temperature, thermal pressure and

Table 1. Properties of the Models

Model	AH	ζ	$t_{\text{t, col}}$ 10^7 s
I	none	-	9.88
IIInl	nonlinear	10%	10.10
IIItu	turbulent	10%	9.89
IIIInl	nonlinear	30%	10.60
IIItu	turbulent	30%	9.93

**Figure 1.** Profiles of (a) temperature for models I (no AH), IIInl (H_{nl} , $\zeta = 0.1$), IIItu (H_{tu} , $\zeta = 0.1$), IIIInl (H_{nl} , $\zeta = 0.3$) and IIItu (H_{tu} , $\zeta = 0.3$) for several evolution times.

β (magnetic to thermal pressure ratio) profiles of our models. These profiles are shown from the beginning of the calculations, throughout the optical phase ($T \leq 10^5 \text{ K}$), until $9.8 \times 10^7 \text{ s}$ (very close to the total collapse time of model I, $9.88 \times 10^7 \text{ s}$). The influence of the AH on the collapse of the perturbed gas can be well understood following the profiles of Figure 1. For model I (with no AH), nearly all the gas contained in the perturbation reaches $\sim 10^4 \text{ K}$ in the

total collapse time of $9.88 \times 10^7 \text{ s}$. All the models with AH have total collapse times longer than this. Comparing the results for nonlinear and turbulent AH models, we can see that nonlinear AH is more effective in inhibiting the development of the collapse than turbulent AH. Note that model IIIInl (nonlinear AH, with $\zeta = 30\%$) has the highest total collapse time, and therefore the smallest amount of “cool” gas when the evolution time reaches $9.8 \times 10^7 \text{ s}$.

As we see from the thermal pressure profiles of Figure 2, as compared to Figure 1, the drop in the temperature causes a reduction in the thermal pressure. This behaviour is a consequence of the fact that the sound crossing time is much longer than the cooling time, so there was no time for repressurizing. The β profiles (Figure 3) show that, at the beginning of the calculations, the magnetic pressure is much smaller than the thermal one; but, as the perturbation evolves, the magnetic pressure becomes more important, as a result of the drop in the temperature of the perturbed gas, β becomes > 1 , and any (slight) compression of the gas will contribute to the increase in β (assuming frozen-in fields, the magnetic field increases according to $B \propto \rho^{2/3}$ for a spherical geometry).

When the temperature falls to $\sim 5 \times 10^5 \text{ K}$, the gas begins to emit optical and UV lines. Before this optical line emitting stage, the gas cooling occurs via EUV and X-rays lines. We have calculated the emissivity of low-ionization optical lines as well as that of high-ionization UV lines. The results of our models may be compared to the observational data from monitoring campaigns, such as those of the Seyfert 1 galaxies Fairall 9 (with *IUE*, Rodríguez-Pascual et al. 1997; in the optical range, Santos-Lleó et al. 1997) and NGC 5548 (Dumont et al. 1998).

We set the beginning of the phase of optical–UV line emission when the temperature of the innermost cell (that is, the first cell to cool) falls below $5 \times 10^5 \text{ K}$. Figure 4 shows the evolution during this phase of the luminosity of the low-ionization line $H\beta$, and of the high-ionization lines $\text{HeII } 1640 \text{ \AA}$, $\text{CIV } 1549 \text{ \AA}$, $\text{Nv } 1240 \text{ \AA}$ and $\text{OVI } 1034 \text{ \AA}$, for the models I, IIInl and IIIInl. The variability pattern of the three models is very similar for all the lines studied. In addition, AH enhances significantly, albeit not strongly, the broad line emission. We should note that the amplitude of variation of the $H\beta$ line is smaller than that of the high-ionization ions, and that the time-scale of its variability is much longer.

With respect to the variability of the collisionally excited high-ionization UV lines, their luminosities show well-defined maxima occurring $\sim 10\text{--}25$ days after the appearance of the first gas with $T < 5 \times 10^5 \text{ K}$. The variability

b)

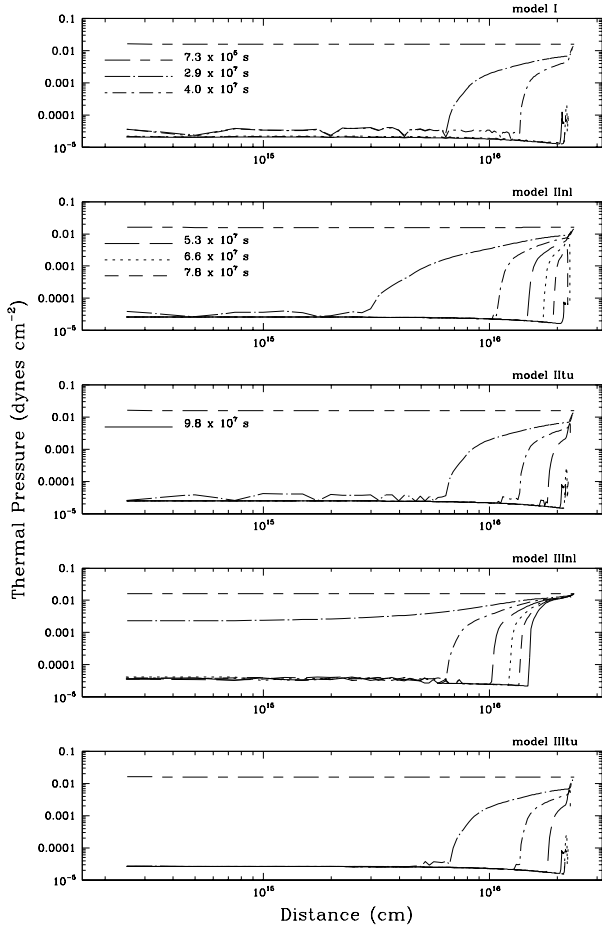


Figure 2. Profiles of (b) thermal pressure for models I(no AH), IIInl(H_{nl} , $\zeta = 0.1$), IIItu(H_{tu} , $\zeta = 0.1$), IIIInl(H_{nl} , $\zeta = 0.3$) and IIIItu(H_{tu} , $\zeta = 0.3$) for several evolution times.

of the lines CIV 1549 Å, Nv 1240 Å and OVI 1034 Å is faster and of larger amplitude than that of the HeII 1640 Å line. For model IIIInl, the time interval $\Delta t_{1/2}$ for the line luminosity to decrease from its maximum value to half-maximum value is 46.0 d, 24.2 d, and 31.9 d, for the lines CIV 1549 Å, Nv 1240 Å and OVI 1034 Å, respectively, whereas for HeII 1640 Å, $\Delta t_{1/2} = 152$ d. Note that, in addition to increase the luminosities of the lines (during the period from the time of peak luminosity and $t = 100$ d, the increase is 30–55% for HeII 1640 Å, 60–70% for CIV 1549 Å, 48–52% for Nv 1240 Å, and 51–60% for OVI 1034 Å) the AH makes the luminosity peaks more prominent.

The evolution of the H β luminosity contrasts with the evolution of the high-ionization UV lines in that it is almost constant within an elapsed time of about 300 days. It shows a broad maximum at 150–200 days and varies within only 10% between 70 and 320 days. The fact that the amplitude of variation of the H β line is smaller than that of the high-ionization ions, and that the time-scale of its variability is much longer is in a first order agreement with observations. For Fairall 9, the H β line shows a smoother pattern of variability than HeII 1640 Å, with a time-lag $\tau_d = 23.0$ d and a

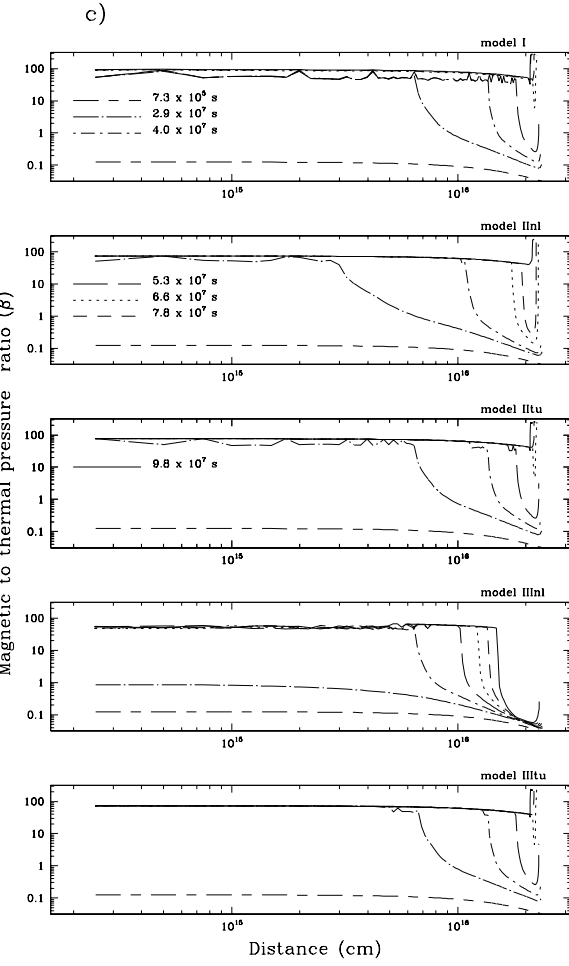


Figure 3. Profiles of (c) magnetic to thermal pressures ratio for models I(no AH), IIInl(H_{nl} , $\zeta = 0.1$), IIItu(H_{tu} , $\zeta = 0.1$), IIIInl(H_{nl} , $\zeta = 0.3$) and IIIItu(H_{tu} , $\zeta = 0.3$) for several evolution times.

ratio of maximum to minimum fluxes $R_{\text{max}} = 1.55$, whereas for HeII 1640 Å, $\tau_d = 4.2$ d and $R_{\text{max}} = 3.25$. However, a closer comparison of the luminosity and time-lags between Balmer and high-ionization lines reveals that the predicted luminosity of H β is too low and its variability too slow. For model IIIInl, at $t = 150$ d, even close to the maximum of the H β line, and far from the maximum of the CIV 1549 Å line, the ratio CIV 1549 Å/H β is 24.7, whereas the typical value for AGN BLRs is ~ 5 . AH does not seem to account for the Balmer recombination lines, which could be explained by photoionization, but it makes a significant contribution, both to the energetics and to the variability of the high-ionization lines.

5 DISCUSSION AND CONCLUSIONS

In our model, the values of the time of the luminosity peak $t_{\text{max}} - t_{\text{max}} = 29.7$ d for CIV 1549 Å, $t_{\text{max}} = 21.9$ d for Nv 1240 Å, and $t_{\text{max}} = 21.9$ d for HeII 1640 Å, for model IIInl — reproduce the observed sequence of time-lags in AGN BLRs, with the time lags for Nv 1240 Å and HeII 1640 Å

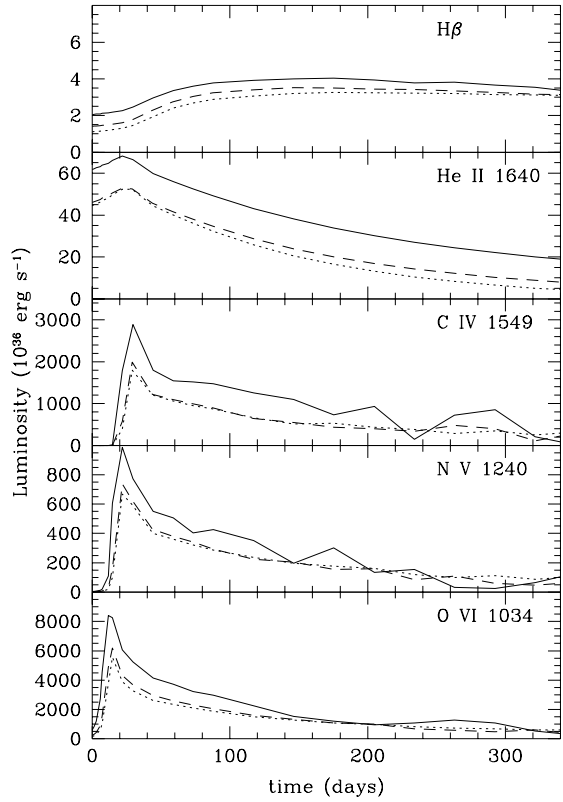


Figure 4. Luminosity variability of the line $H\beta$, as well as those of the UV high-ionization lines $HeII\ 1640\ \text{\AA}$, $CIV\ 1549\ \text{\AA}$, $NV\ 1240\ \text{\AA}$ and $OVI\ 1034\ \text{\AA}$, for models I (dotted lines), IIInl (dashed lines) and IIIInl (solid lines). The time is counted from the beginning of the optical phase (i.e. when T becomes $< 5 \times 10^5\ \text{K}$).

being of comparable magnitude and shorter than those of $CIV\ 1549\ \text{\AA}$ (our models predicts an even shorter variability time scale for $OVI\ 1034\ \text{\AA}$: $t_{\max} = 11.7\ \text{d}$ for model IIIInl). The usual interpretation is that the $HeII$ – NV emission region is located at a shorter distance from the central continuum source than the $CIV\ 1549\ \text{\AA}$ region — in the case of NGC 5548, at 6 and 10 light-days, respectively — (Dumont et al. 1998). The present results suggest that at least part of this trend could be due to different evolutionary time scales for each line within one single cloud or cloud ensemble at one given position with respect to the central source, instead of different clouds giving rise predominantly to different lines at differing locations.

We can interpret our results in the light of the discussions by Dumont et al. (1998), which, although give support to scenario in which the BLR consists at least of two different regions, in which low- and high-ionization lines are predominantly produced, also point out some inconsistencies of the photoionization models based in this scenario with respect to the energy budget, the line ratios and the line variability. The variability represents the greater challenge for the stratified model for the formation of the high- and low-ionization lines, in which the more ionized lines are formed closer to the center ($CIV\ 1549\text{\AA}$ and $HeII\ 1640\text{\AA}$) and the less ion-

ized further out (Collin-Souffrin et al. 1986; Collin-Souffrin, Hameury & Joly 1988).

It is possible that the standard stratified model suffers of an excessive number of emission regions. For NGC 5548, Dumont et al. (1998) distinguishes four zones: the $MgII$ – $CIII]$ emission zone, at ~ 30 – 50 lt-days; the Balmer lines– HeI emission zone, at ~ 12 – 20 lt-days; the $Ly\alpha$ – CIV emission zone, at 8 – 12 lt-days; the NV – $HeII$ emission zone, at 4 lt-days. Our results also allow for several locations for the formation of the broad lines, with the high-ionization lines being produced closer to the central continuum source, and having an important contribution from AH, and the Balmer lines being produced at a more distant location, and powered mostly by photoionization, which would be responsible for most of its variability. Of course, some fraction of the broad-line spectrum could be non-variable, and the AH-powered clouds could contribute to a slowly-variable part of the Balmer lines emission. The AH mechanism would be one more ingredient in the constitution of the time-lags. The decreasing values of t_{\max} for the lines $CIV\ 1549\ \text{\AA}$, $NV\ 1240\ \text{\AA}$ and $OVI\ 1034\ \text{\AA}$ shows that different time lags do not necessarily indicate different line formation regions. A stratified model simpler than the standard one could consider the formation of the low-ionization lines in clouds far from the center accommodate the production of the highest ionization lines (from $CIV\ 1549\ \text{\AA}$ to $OVI\ 1034\ \text{\AA}$) in the same location very close to the center (e.g. in the case of NGC 5548, in the few inner lt-day), with part of delay of the lines with respect to fluctuations of the continuum arising from evolutionary effects within the clouds, and heated/excited by non-radiative processes, in our case, by AH.

The use of Alfvén heating in our models is not aimed at solving all the problems pointed out by Dumont et al (1998): the ‘energy budget problem’, the ‘line ratio problem’ and the ‘line variation problem’. For example, AH is no solution to the ‘energy budget problem’, because of the small contribution of AH to $H\alpha$ emission (and to the Balmer series). However, AH alleviates the ‘line variation problem’ because it reproduces the trend of time lags with different ionization lines, with no need for an excessive stratification of clouds emitting different lines. Although AH does not account for the Balmer recombination lines, which could be explained by photoionization, it makes a significant contribution both to the energetics and to the variability of the high-ionization lines. What we explored here is the possibility that several species of high-ionization lines, are produced at the same location, however, being not only photoionized but also heated/excited by, in the present case, Alfvénic heating.

The lag between continuum and line variability could arise from some process associated with maxima in the continuum emission initiating the collapse. A possible mechanism for triggering the collapse of the perturbation is Compton cooling. Compton cooling resulting from luminous QSOs in clusters of galaxies has been shown to be able to induce or sustaining cooling flows (Fabian & Crawford 1990; Atuko et al. 1998). Compton cooling can also be important in accretion disks (Esin 1997). Mathews and Ferland (1987) find that the Compton temperatures appropriate to quasar spectra are in the range $2.8 \times 10^6 < T_C < 4.6 \times 10^7\ \text{K}$. If the source radiation is soft ($T_C < T_m$, the temperature of the intercloud medium), burst in the central continuum could

induce cooling on time scales close to the Compton cooling time:

$$t_C = \frac{\frac{3}{2} n k_B T_m}{4 \frac{k_B \sigma_T}{m_e c} \frac{L_{\text{bol}}}{4 \pi R^2} n (T_m - T_C)} = \frac{3}{2} \pi \frac{m_e c^2}{\sigma_T} \frac{R^2}{L_{\text{bol}}} (1 - \frac{T_C}{T_m})^{-1},$$

where R is the distance to the source and L_{bol} is its bolometric luminosity (and the other symbols have their usual meaning). For typical values of R and L_{bol} in AGN BLRs,

$$t_C = 4.06 \frac{(R/30 \text{ light days})^2}{(L_{\text{bol}}/10^{47} \text{ erg s}^{-1})} (1 - \frac{T_C}{T_m})^{-1} \text{ days},$$

so it is feasible to induce collapse of perturbations on the required short time scales.

As mentioned in section 2, high amplitude waves cause nonlinear couplings and the nonlinear Alfvénic energy is, in general, converted into thermal energy. The nonlinear damping rate (eq. (1)) is a function of $\bar{\omega}$, which can be written in terms of the ion-cyclotron frequency, $\bar{\omega} = F\omega_{ci}$. We assume $F = 0.1$, which is consistent with laboratory experiments on heat transport in magnetized plasmas. In a electron beam experiment (Burke et al. 1998), classical conduction is observed for the first 2 ms since beam turn-on, after which fluctuations with frequencies $\sim 0.1\omega_{ci}$ spontaneously grow, and at 3 ms, large amplitude fluctuations with frequencies $0.02\omega_{ci}$ appear. Following equation (1), the damping length $L_{\text{damp}} = v_A/\Gamma$ can be written as

$$L_{\text{damp}} = 1.92 \times 10^7 \left(\frac{\xi}{5} \right)^{-1} \left(\frac{\rho \langle \delta v^2 \rangle}{B^2/8\pi} \right)^{-1} F^{-1} n_H^{-1/2} \beta^{1/2} \text{ cm.}$$

For the onset of the AH ($\beta = 1$, $n_H = 5 \times 10^6 \text{ cm}^{-3}$), assuming $\xi = 5$, $\rho \langle \delta v^2 \rangle / (B^2/8\pi) = 1$, and $F = 0.1$, $L_{\text{damp}} = 8.7 \times 10^4 \text{ cm}$, much smaller compared with the initial dimension of the system ($5 \times 10^{16} \text{ cm}$) and the radius where the Alfvénic heating is acting ($4.2 \times 10^{15} \text{ cm}$ for the model IIIInl). This implies that the waves are damped very rapidly and so must be generated locally in the cloud. We have evidence for generation in situ of Alfvén waves from observations of outward and inward fluctuations propagation in the solar wind (Coleman 1968; Belcher & Davis 1971). Roberts et al. (1987) using data from Helios and Voyager spacecraft, investigated the origin and evolution of low-frequency planetary fluctuations from 0.3 to 20AU. They concluded that the outward traveling fluctuations are predominantly generated by the Sun, but that in situ turbulence, most likely due to stream shear, generates fluctuations with both inward and outward senses of correlation. This mixed state provides stronger evidence for in situ generation. We assume that the above scenario can be applied to the BLR clouds allowing the in situ generation of Alfvén waves.

It would be interesting to compare the results of the present model with other models assuming local heating sources. Besides photoionization model by central continuum, local emission models have also been proposed in order to explain the $H\alpha$ luminosities and the major line ratios of cluster nebulae (Voit et al. 1994). The major difference between the work of Voit et al. (1994) and the present one is that we are dealing with an evolutionary model where the heating source is non-radiative (AH heating) and the total pressure includes both thermal and magnetic pressures. On the other hand, in the model of Voit et al. (1994) it is assumed a pressure and heating-cooling equilibrium, while our

model is time-dependent and does not assume any equilibrium. Moreover, Voit et al. (1994) present the results of a photoionization code (CLOUDY), considering the soft X-ray/EUV radiation field of a cooling flow in which cold clouds are embedded, while we restricted ourselves to purely collisional emissivity calculations.

Our model is not aimed at reproducing the continuum emission of any particular AGN. Instead is a tool to investigate separately from photonization effects the role of magnetic fields (magnetic pressure and Alfvén heating) as a mechanism contributing to the delay between the continuum variability and the line variability. A complete model for the BLRs would include photoionization, shocks and magnetic effects. The focus of the present work is on the third ingredient.

We should also note that even non-standard radiative heating mechanisms deserve proper consideration. If the hot intercloud medium is turbulent, mixing layers are expected to develop around the colder BLR clouds. In the conditions of cooling flows, Begelman & Fabian (1990) have shown that EUV radiation from mixing layers could power the line emission of optical filaments in cooling flows. It is possible that, also in BLRs, the radiation from mixing layers around the BLR clouds could constitute an additional, local, photoionization source, besides the central continuum.

Other issue is the stability of the BLR cold clouds. Several external forces are expected to be acting on (and against) the BLR clouds in the harsh environment constituted by the intercloud medium — high temperatures ($T \sim 10^{7-8} \text{ K}$), high relative velocities (up to $\approx 10^4 \text{ km s}^{-1}$), and, probably, turbulence. Significant motions of the BLR clouds relative to the intercloud medium could lead to disruption of the clouds, and radiation forces could ablate the protoclouds before they contribute fully to the broad line emission (Mathews & Doane 1990). Also with respect to this topic, magnetic fields have a role to play, providing supporting pressure and confinement of the clouds (Rees 1987; Gonçalves et al. 1993, 1996). In addition, in the motion of the BLR clouds through the whole of BLR (with the accompanying effects on the line profiles) magnetic fields could have a dynamical role, as it seems to the case in cooling flows (Gonçalves & Friaça 1999). Finally, in order that the density reaches values high enough to account for the absence of forbidden lines in AGN BLRs, some process should remove the magnetic field in the late evolution of the perturbations, when pressure equilibrium has been achieved, otherwise the magnetic field would prevent further compression of the BLR cloud. One mechanism that was shown to be effective in optical filaments in cooling flows is magnetic reconnection (MR) (Jafelice & Friaça 1996, Friaça & Jafelice 1999). Therefore, it would be interesting to investigate MR in BLR clouds, both as a heating source and as mechanism for removing magnetic support.

Acknowledgements

We are grateful to R. Mewe for making us available the MEKA code and its atomic database. We thank the anonymous referee for his/her comments, which helped us to significantly improve the paper. DRG would like to thank the grant of the Brazilian agency FAPESP (98/7502-0) and the Spanish DGES PB97-1435-C02-01 grant. ACSF and

VJP would like to thank the Brazilian agency CNPq for partial support. We also acknowledge partial support by Pronex/FINEP (41.96.0908.00).

REFERENCES

Atuko N., Habe A., Isibasi N., 1998, MNRAS, 295, 632

Baldwin J.A., 1997, in Emission Lines in Active Galaxies: New Methods and Techniques, IAU Col. 159, eds. B.M. Peterson, F.-Z. Cheng and A.S. Wilson, ASP Conference Series, 113, p. 80

Begelman M.C., Fabian A.C., 1990, MNRAS, 244, 26

Belcher J. W., Davis, L., 1971, J. Geophys. Res., 76, 3534

Burke A. T., Maggs J. E., Morales G. J., 1998, PRL, 81, 3659

Chin Y., Wentzel D. G., 1972, Ap&SS, 16, 465

Cloutman L. D., 1980, Los Alamos Report. LA-8452-MS

Coleman P. J., 1968, ApJ, 153, 371

Collin-Souffrin S., Joly M., Pequignot D., Dumont S., 1986, A&A, 166, 27

Collin-Souffrin S., Hameury J. M., Joly M., 1988, A&A, 205, 19

Contini M., Viegas-Aldrovandi S., 1990, ApJ, 350, 125

David L. P., & Bregman J. N., 1989, ApJ, 337, 97

David L. P., Bregman J. N., & Seab C. G., 1988, ApJ, 329, 66

dos Santos L. C., Jatenco-Pereira V., Opher R. 1993, ApJ, 410, 732

Dumont A. M., Collin-Souffrin S., Nazarova L., 1998, A&A, 331, 11

Espey B., 1997, in Emission Lines in Active Galaxies: New Methods and Techniques, IAU Col. 159, eds. B.M. Peterson, F.-Z. Cheng and A.S. Wilson, ASP Conference Series, 113, p. 175

Esin A.A., 1997, ApJ, 482, 400

Fabian A.C., Crawford C.S., 1990, MNRAS, 247, 439

Friaça A. C. S., 1986, A&A, 164, 6

Friaça A. C. S., 1993, A&A, 269, 145

Friaça A. C. S., Jafelice L. C., 1999, MNRAS, 302, 491

Friaça A. C. S., Gonçalves D. R., Jafelice L. C., Jatenco-Pereira V., Opher R., 1997, A&A, 324, 449

Gonçalves D. R., Friaça A. C. S., 1999, MNRAS, 309, 651

Gonçalves D. R., Jatenco-Pereira V., Opher R., 1993a, Paper I, ApJ, 414, 57

Gonçalves D. R., Jatenco-Pereira V., Opher R., 1993b, A&A, 279, 351

Gonçalves D. R., Jatenco-Pereira V., Opher R., 1996, Paper II, ApJ, 463, 489

Gonçalves D. R., Jatenco-Pereira V., Opher R., 1998, ApJ, 501, 797

Grevesse N., Anders E., 1989, Cosmic Abundances of Matter. Am. Inst. Phys., ed. C.J. Waddington, New York, p. 183

Hollweg J. V., 1986, J. Geophys. Res., 91, 4111

Hollweg J. V., 1987, ESA, in Proc. 21st ESLAB Symp. on Small-Scales Plasma Processes in Solar Chromosphere Corona, Interplanetary Medium and Planetary Magnetospheres, p. 161

Jafelice L. C., Friaça A. C. S., 1996, MNRAS, 280, 438

Jatenco-Pereira V., & Opher R., 1989a, A&A, 209, 327

Jatenco-Pereira V., & Opher R., 1989b, MNRAS, 236, 1

Jatenco-Pereira V., & Opher R., 1989c, ApJ, 344, 513

Jatenco-Pereira V., Opher R., & Yamamoto L. C., 1994, ApJ, 432, 409

Kaburaki O., Uchida Y., 1971, PASPJ, 23, 405

Krolik J. H., 1988, ApJ, 325, 148

Krolik J. H., McKee C. F., & Tarter C. B., 1981, ApJ, 249, 422

Lagage P. O., Cesarsky C. J., 1983, A&A, 125, 249

Mathews W. G., Doane J. S., 1990, ApJ, 352, 423

Mathews W. G., Ferland G. J., 1987, ApJ, 323, 456

Mewe R., Gronenschield E. H. B., van der Oord G. H. J., 1985, A&AS, 62, 197

Netzer H., 1990, in Active Galactic Nuclei, ed. J.J.-L Courvoisier and M. Mayor (Berlin: Springer-Verlag)

Opher R., & Pereira V. J. S., 1986, Astrophys. Lett., 25, 107

Priest E. R., 1994, in Plasma Astrophysics, ed. J.G. Kirk, D.B. Melrose and E.R. Priest (Berlin: Springer-Verlag), p. 38

Pistinner S., Levinson A., & Eichler D., 1996, ApJ, 467, 162

Rees M. J., 1984, ARA&A, 22, 471

Rees M. J., 1987, MNRAS, 228, 47

Roberts D. A. et al., 1987, J. Geophys. Res., 92, 12023

Rodríguez-Pascual P. M., et al., 1997, ApJS, 110, 9

Rychtmyer R. D., & Morton K. W., 1967, in Difference Methods for Initial Value Problems, Interscience, New York

Santos-Lleo M., et al., 1997, ApJS, 112, 271

Spitzer L., 1956, in Physics of Fully Ionized Gases, Interscience, New York

Tscharnutter W. M., Winkler K. H., 1979, Comp. Phys. Comm., 18, 171

Tu C. Y., Pu Z. Y., Wei F. S., 1984, J. Geophys. Res., 89, 9695

Uchida Y., Kaburaki O., 1974, Sol. Phys., 35, 451

Vasconcelos M. J., Jatenco-Pereira V., & Opher R., 2000, ApJ, 534, 967

Voit G. M., Donahue M., & Slavin J. D., 1994, ApJ, 95, 87

Wentzel D. G., 1974, Sol. Phys., 39, 129